DIGITAL MULTICHANNEL BIOIMPEDANCE ANALYSER: SIGNAL PROCESSING APPROACHES

A. Ronk*, P. Annus,** A. Kuusik*, R. Land* and O. Märtens*

* Department of Electronics, Tallinn University of Technology, Tallinn, Estonia
** Competence Centre ELIKO, Tallinn, Estonia

ronk@ttu.ee

Abstract: Measurement of electrical bioimpedance enables to characterize a state of tissues/organs, to get diagnostic images, to find hemodynamical parameters, etc. In this paper we consider two ways for processing signals in a digital multichannel bioimpedance analyser developed for monitoring of the state of a working heart.

Introduction

Measurement of electrical bioimpedance enables to characterize a state of tissues/organs, to get diagnostic images, to find hemodynamical parameters, etc. [1-3]. In this paper we consider two ways to process signals in a digital multichannel bioimpedance analyser developed for monitoring of the state of a working heart [4].

Materials and Methods

A simplified block diagram of the developed digital multichannel bioimpedance analyser (DMBA) is presented in Fig. 1.

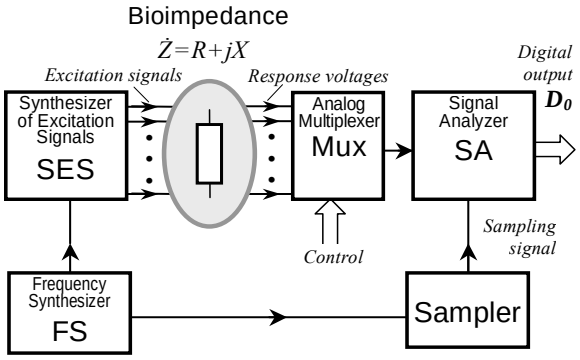

Figure. 1. Block diagram of the DMBA.

In the DMBA eight sinusoidal excitation currents of eight frequencies f_e are formed and simultaneosly sent to one, two or four excitation electrodes put in the heart. In case of two/four electrodes the excitation frequencies form four/two groups of close (but different) values and enable thus to compare the frequency responses to the excitations from different electrodes.

One, two or four measurement electrodes receive summary responses to all the excitations. Every response is a sum of eight excitations modulated by slowly varying bioimpedances $\dot{Z}(f_e)$ (which include heart-beat and breathing components) and a slowly varying offset (caused by bioelectrical activity of the heart).

The complex bioimpedances $\dot{Z} = R + jX = M \cdot e^{j\Phi}$ are measured for all the 4×8 tissue/frequency channels (between different electrode pairs at eight frequencies from 1 or 10 kHz up to 1 MHz) with a frequency $f_0 = 1\,\text{kHz}$.

The excitation frequencies f_e and also the sampling frequencies f_s are chosen to be integer multiples of f_0. As in the developed DMBA the whole signal path from the generation of the set of excitation signals to the A/D conversion procedure and data analysis is synchronous by design, optimised signal processing methods can be applied. The frequency components of the entire test signal are designed to meet the endpoint discontinuity requirements and are therefore well suited for direct discrete Fourier analysis without applying preceding windowing procedure and also for synchronous detection.

The complex values of bioimpedance $\dot{Z}$ can be found for the excitation frequencies $f_e = n_e f_0$ processing the responses from the measurement electrodes in two basic ways, which both use undersampling (aliasing) and sparsity of the excitation/response spectrum. Let us consider these approaches and the accompanying restrictions for the values of the excitation and sampling frequencies.

Fourier transform based solution.

This solution applies well-known discrete Fourier transform (DFT). Arbitrary desired $\dot{Z}(f_e)$ is found in result of a direct discrete Fourier transform of the response (of the frequency f_0) as the n_e th Fourier coefficient (if $f_e < f_s / 2$) or as a Fourier coefficient which is made nonzero by just one nonzero aliasing component (if $f_e > f_s / 2$). It is evident, that in such a case the choice of excitation frequencies is restricted: their ratios must have properly chosen values. A more restricted choice of the excitation and sampling frequencies (their ratios) allows us to find $\dot{Z}$ for all f_e as Fourier coefficients of fixed (or even consecutive) numbers.

ISSN: 1727-1983

The DFT is performed so that only the (nonzero) coefficients for the used excitation frequencies are computed. In case of single-point DFT the analysis frequency always matches the input frequency and only the energy at one frequency bin of the DFT spectrum is looked. As a result, the amount of computations is reduced. Analogous approach is used in the commercially available impedance converter network analyser AD5933 [5].

This approach has been implemented in the first version of the developed DMBA.

The recursive Fourier transform (RFT) [6,7] is applicable too, but we have not considered this possibility in detail.

Synchronous detection based solution.

In this case $\dot{Z}(f_e)$ is found for every tissue/ frequency channel applying a pair of synchronous detectors, which both sum N_e samples with periodically changed signes over $T_0 = 1/f_0$ to compute real and imaginary parts $R(f_e)$ and $X(f_e)$ of the bioimpedance $\dot{Z}(f_e)$ on the basis of the found two sums $s_{re,e}$ and $s_{im,e}$ as follows:

$$R(f_e) = s_{re,e} \cdot C_e \quad \text{and} \quad X(f_e) = s_{im,e} \cdot C_e \qquad (1)$$

where

$$C_e = C_{w,e} / N_e \qquad (2)$$

and $C_{w,e}$ is a waveform coefficient determined by the ratio f_s / f_e .

Such signal processing is applicable, if the excitation and sampling frequencies satisfy certain restrictions:

1) The lowest-frequency excitations of the electrodes 1, 2, 3 and 4 are e.g. the 10th, 11th ,12th and 13th Fourier components of the summary excitation of the frequency $f_\Sigma \geq f_0$ (difference of the 1st level frequencies must be below the desired 10%, every chosen component number must have a unique divider) and the higher-frequency excitations (of the levels $l = 2,3,..., L$) can be the Fourier components of $(2 \cdot I)^{l-1}$ times higher numbers, where the odd integer I can be 1 but not any other divider of the chosen component numbers (10, 11, 12, 13).
2) L pairs of detectors, which find $\dot{Z}$ at the frequencies of L excitation signals of one excitation electrode, work using a common uniform sample train. The frequency of this train is $2^{L+1}/J$ times higher than the electrode's lowest excitation frequency. The undersampling factor, i.e. the odd integer $J < f_\Sigma / f_0$ can be 1, but not any other divider of the chosen component numbers. A union of such sample trains can be considered as a summary nonuniform (but periodic) sample train.

Let us assume that N_e last subsequent summary response values are stored in the array V so that after fullfilling the array ($V(i)$ in the order $i = 1,2,..., N_e$) always the oldest element value $v_{old} = V(i_{old})$ is read out and replaced by the next new summary response value $V(i_{old}) = v_{new}$. After that if $i_{old} = N_e$ then i_{old} is set equal to 1, otherwise $i_{old} = i_{old} + 1$ (initial $i_{old} = 1$ and initial values of V are zeros).

Let us assume also that we have found the sum s_e of N_e latest values stored in $V(i)$ which were taken for summing with appropriate sign ($+$ or $-$). Then the new sum of N_e latest values in V can be found as

$$s_{e,new} = s_{e,old} \pm (v_{new} - v_{old}) \qquad (3)$$

where the sign ($+$ or $-$) is determined by i_{old} and by corresponding frequencies f_e, f_s and f_0 (of course, the sign changes are in quadrature for computing real and imaginary parts of $\dot{Z}(f_e)$).

Thus, in order to obtain a new value $\dot{Z}(f_e)$ for one tissue/frequency channel at every sampling step, one has to perform at every step only two operations (3) to find the sums $s_{re,e}$ and $s_{im,e}$, and the multiplications (1).

On the other hand, if noise suppression of the considered here approach appears to be insufficient, then it is possible to choose one of the two next ways to improve it:

1) The values $s_{re,e}$ and $s_{im,e}$ (found for computing $\dot{Z}(f_e)$) can be stored in two separate arrays of the length $N_{av,e}$ like the measurement signal values in V and also processed in the same way. As a result, the latest $N_{av,e}$ sums can be averaged at an abitrary sampling interval for further finding averaged values of $R(f_e)$ and $X(f_e)$ according to (1);
2) The currently found sums $s_{re,e}$ and $s_{im,e}$ can be used to produce at every sampling step the averaged values of such sums s_e according to

$$\tilde{s}_{e,new} = \alpha_e \tilde{s}_{e,old} + (1 - \alpha_e) s_{e,new} \qquad (4)$$

where $s_{e,new}$ is a new (current) sum, a properly chosen $\alpha_e < 1$ is close to 1 and the first average value $\tilde{s}_{e,new}$ .is set equal to $s_{e,new}$ (the initial $\tilde{s}_{e,old} = s_{e,new}$). These averaged values $\tilde{s}_{re,e}$ and $\tilde{s}_{im,e}$ can be used in (1) to obtain the desired results..

In both concidered solutions the offset is found as a direct component of the measurement signal.

ISSN: 1727-1983

Results and discussion

Simulations and the first tests have shown that the described signal processing methods work. The Fourier transform based approach suits better for DSP solutions, the synchronous detection based approach seems attractive for specialized low-power ASIC solutions.

In order to obtain information about real problems (disturbances, distortions) and to find the most practical way for signal processing, the first version of the analyser has been realised. This version applies discrete Fourier transform and it has been tested in close-to-real working conditions. In result of the first tests we can state the following:

1) Realization of A/D conversion appeared to be the main bottle-neck, which did not allow us to use in case of 1, 2 and 4 measurement electrodes (1, 2, and 4 multiplexed responses) sampling frequencies over 800, 400 and 200 kHz correspondingly.
2) Even at these maximal sampling frequencies the noise suppression achieved by means of the discrete Fourier transformation was not good enough. The noise masked the small (from fraction up to some per cent) modulations caused by the varying bioimpedance. Thus we had to introduce into the DMBA (in Fig.1) first order analog low-pass filters for conditioning the measurement signals and also a digital compensation of the analog filter's frequency response. In this way a sufficiently low noise level was achieved at the output.

The detailed description of this analyser version and the final test results can not be presented yet.

As we wanted to compare noise suppression capabilities of the discrete Fourier transform and the synchronous detection, we simulated analysis of an 8-component test signal with added offset and Gaussian white noise. Processing of the test signal, which consists of sinusoidal components of the frequencies 1, 2, 4, 8, 16, 32, 64 and 128 kHz, at the sampling freguency 512 kHz showed (see Fig. 2, a) and b)) that the mentioned methods both resulted the same noise level and highly correlated noise for every identified sinusoidal component (its parameters: amplitude, phase, real and imaginary parts). Thus, the considered approaches are equivalent in this aspect.

The synchronous detection based approach needs less computations than the DFT based approach, even more: it enables to obtain much more easily the desired results at every sample and (applying the described here averaging methods) also the averaged results with lower noise level (see the results in Fig. 2, c) and d)). However, at present we have to prefer the DFT based approach.

The SD based approach suits well for a system with M simultaneously working SISO (single input – single output) tissue impedance measurement channels and eliminates interference between these channels. It suits also for alternating (cyclic) measurement of responses to the excitations from M inputs at every output. But a sufficiently good detailed solution for a MIMO measurement system, i.e. for simultaneous measurement of all these M responses at every measurement electrode, has to be found yet.

Conclusions

The obtained results allow us to state that the considered DFT based approach seems to be good enough for signal processing in the DMBA of the realised hardware solution (see Fig. 1, more details in [4]) where computations are performed in a DSP.

If we succeed in finding efficient algorithmic and (expectedly) ASIC solutions for the SD approach based signal-processing channel(s) of a MIMO system then the MIMO system becomes computationally much simpler and it can be realised without using any DSP.

References

[1] McAdams, E. T., Jossinet, J. (1995): 'Tissue impedance: a historical review', *Physiological Measurements*, vol. 16, pp. A1-A13.

[2] Gersing, E. (1998): 'Impedance spectroscopy on living tissue for determination of the state of organs', *Bioelectrochemistry & Bioenergetics*, vol. 45, pp. 145-149.

[3] Salo, R. W. (2003): 'Application of impedance volume measurement to implantable devices', *Int. Journal of Bioelectromagnetism,* vol. 5, no. 1, pp. 57–60.

[4] Min M. et al. (2004): 'A sampling multichannel bioimpedance analyzer for tissue monitoring', Proc. of 26th Conf. IEEE Eng. in Medicine & Biology Society, Sept. 1-5, 2004, San Francisco, USA, pp. 902-905.

[5] Analog Devices, Internet site address: http://www.analog.com/UploadedFiles/Data_Sheets/272777363AD5933_prb.pdf (Sept. 2005)

[6] Hostetter, H., (1980): 'Recursive discrete Fourier transformation', *IEEE Trans. Acoustics, Speech, and Signal Processing,* vol. 28, no. 2, pp. 184-190.

[7] Várkonyi-Kóczy, A. R., (1995): 'A recursive fast Fourier transformation algorithm', *IEEE Trans. Circuits and Systems – II: Analog and Digital Signal Processing,* vol. 42, no. 9, pp. 614-616

Acknowledgement

This work was supported by the Estonian Science Foundation under the grants 5897 and 5902. Practical implementation was financed by the Enterprise Estonia (EAS) through the Competence Centre ELIKO.

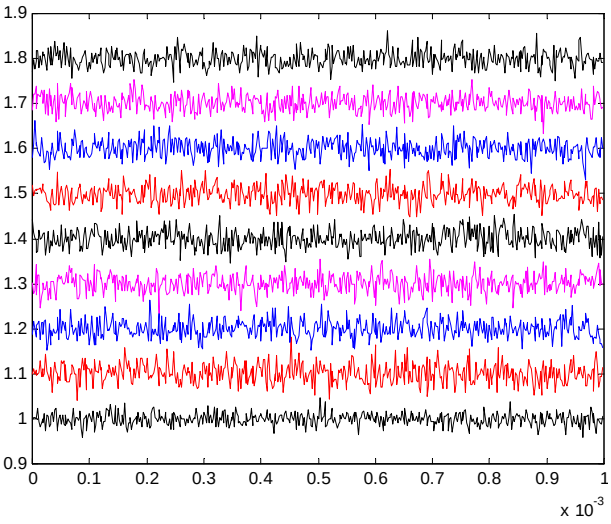

a) Results of synchronous detection (SD) applying (3)

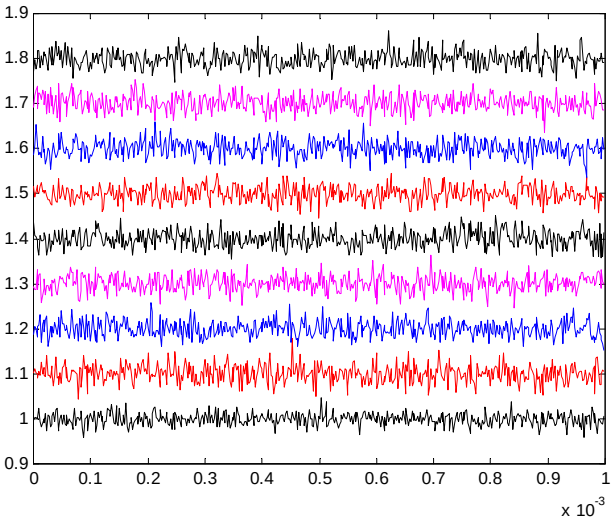

b) Results of discrete Fourier analysis (DFT)

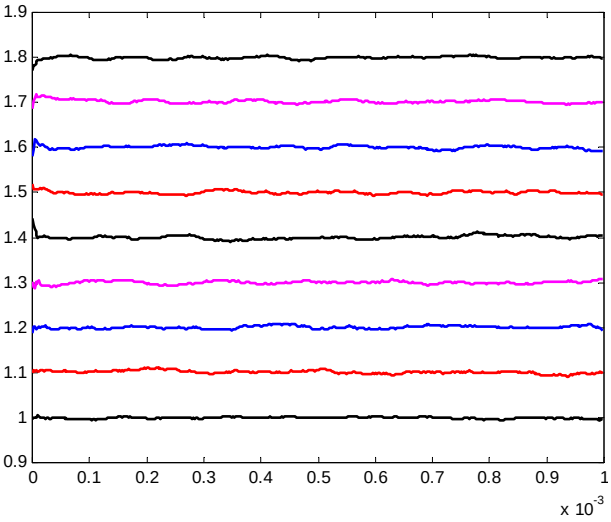

c) SD results averaged over $N_{av,e} = 32$ last values

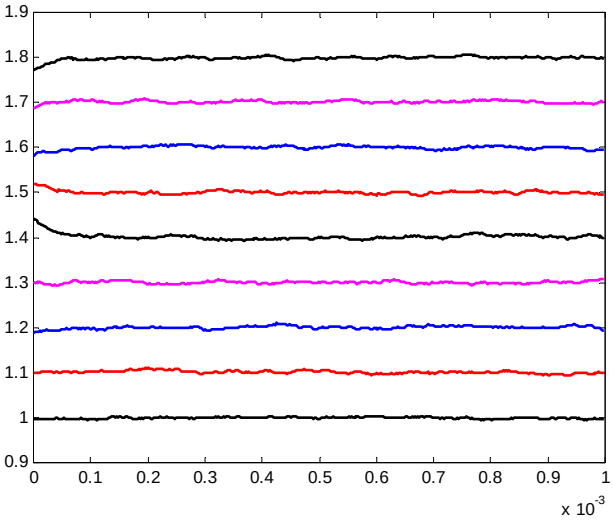

d) SD results averaged applying (4) with $\alpha = 0.95$

Figure 2. Computed offset and amplitudes of sinusoidal componets of the test signal, which consists of components of the frequencies 1, 2, 4, 8, 16, 32, 64 and 128 kHz with corresponding amplitudes 1.1, 1.2, 1.3, 1.4, 1.5, 1.6, 1.7 and 1.8. The offset of the constant value 1 and Gaussian white noise were added to the test signal. The used sampling frequency was 512 kHz. The results are presented for 512 samples of the second measurement cycle of the length $T_0 = 1/f_0 = 1$ msec (thus, the plots c) and d) demonstrate transients of used different averaging processes).

ISSN: 1727-1983